Cement & Concrete Composites 30 (2008) 831–838

Contents lists available at ScienceDirect

Cement & Concrete Composites

journal homepage: www.elsevier.com/locate/cemconcomp

Preparation of C200 green reactive powder concrete and its static–dynamic behaviors

Zhang Yunsheng *, Sun Wei, Liu Sifeng, Jiao Chujie, Lai Jianzhong

Jiangsu Key Laboratory for Construction Materials, Southeast University, Nanjing 210096, PR China

ARTICLE INFO

Article history:
Received 30 April 2006
Received in revised form 14 June 2008
Accepted 16 June 2008
Available online 27 June 2008

Keywords:
C200
Green reactive powder concrete (GRPC)
Static mechanical behavior
Dynamic tensile behavior

ABSTRACT

In this paper, a new type of green reactive powder concrete (GRPC) with compressive strength of 200 MPa (C200 GRPC) is prepared by utilizing composite mineral admixtures, natural fine aggregates, short and fine steel fibers. The quasi-static mechanical properties (mechanical strength, fracture energy and fiber–matrix interfacial bonding strength) of GRPC specimens, cured in three different types of regimes (standard curing, steam curing and autoclave curing), are investigated. The experimental results show that the mechanical properties of the C200 GRPC made with the cementitious materials consisting of 40% of Portland cement, 25% of ultra fine slag, 25% of ultra fine fly ash and 10% of silica fume, 4% volume fraction of steel fiber are higher than the others. The corresponding compressive strength, flexural strength, fracture energy and fiber–matrix interfacial bonding strength are more than 200 MPa, 60 MPa, 30,000 J/m^2 and 14 MPa, respectively. The dynamic tensile behavior of the C200 GRPC is also investigated through the Split Hopkinson Pressure Bar (SHPB) according to the spalling phenomena. The dynamic testing results demonstrate that strain rate has an important effect on the dynamic tensile behavior of C200 GRPC. With an increase of strain rate, the peak stress rapidly increases in the dynamic tensile stress–time curves. The C200 GRPC exhibits an obvious strain rate stiffening effect in the case of high strain rate. Finally, the mechanism of excellent static and dynamic properties gains of C200 GRPC is also discussed.

1. Introduction

Reactive powder concrete (RPC) is an advanced cement based material, which originally developed in the early 1990s by Bouygues' laboratory in France [1]. RPC possess ultra-high static and dynamic strength, high fracture capacity, low shrinkage and excellent durability under severe condition [1–4]. The microstructure of RPC is optimized by precise gradation of all particles in the mix to yield maximum compactness [5–11]. With these merits, RPC has a great potential prospect in the protective shelter of military engineering and nuclear waste treatment, which has received significant concerns from experts across the word [12–14]. However, the high cost, complex fabrication technique and high energy demand of RPC severely limit its commercial development and application in the practical engineering [12,15,16].

It is well known that the major components of RPC commonly used across the world include Portland cement, ultra fine quartz powder (⩽600 μm), silica fume (accounting for 25% or greater weight of the total binders) and small sized steel fibers [17]. Obviously, these expensive raw materials are responsible for the high production cost. In addition, the rigorous curing regimes usually employed in the production of RPC (200 °C autoclave curing or 90 °C heating curing) result in a very low producing efficiency and high energy consumption [18,19]. Therefore, how to increase the ratio of performance to cost is a key problem for the application of RPC in practical engineering.

In order to reduce the production cost of RPC, 50–60% of Portland cement is replaced by the cheap composite mineral admixtures that consist of two or three types of components such as fly ash, slag, and a small dosage of silica fume (10%) in this study. The ultra fine quartz sand with the maximal diameter of 600 μm is totally replaced by the least costly and easily obtained natural river sand with the maximal diameter of 3 mm. A short and fine steel fiber with much lower price ($2500 per ton) than the one used by France is specially designed and manufactured in Guo Mao steel fiber company in Jiang Xi Province, PR China. In addition, three different curing regimes: standard curing (20 °C and 100% RH) with low energy consumption, steam curing (90 °C heating curing) with medium energy consumption, and autoclave curing (200 °C and 1.7 MPa pressure) with high energy consumption, are systematically investigated to explore the feasibility of less energy-intensive curing regimes for preparing a novel type of green reactive powder concrete with compressive strength of 200 MPa (C200 GRPC).

In the past several decades, there has been an increasing interest in investigating the effect of strain rates on the mechanical

* Corresponding author.
E-mail address: zhangys279@163.com (Z. Yunsheng).

0958-9465/$ - see front matter © 2008 Elsevier Ltd. All rights reserved.
doi:10.1016/j.cemconcomp.2008.06.008

behavior of concretes under high speed impact load. However, most dynamic tests in the open literatures are related to dynamic compression. In fact, the destruction of concrete structures subjected to high speed impact loading is mainly attributed to a low dynamic tensile strength of the concrete, rather than a lack of dynamic compressive strength. So it is very important to study the dynamic tensile behavior of concrete. However, little literature is available on dynamic tensile behavior of concrete due to the stress concentration and load eccentricity in conducting dynamic tensile tests [20–23]. In order to solve these problems, a tensile wave reflected from the incident compressive one at the free surface of concrete specimen by using Split Hopkinson Pressure Bar (SHPB) is used to study the dynamic tensile behavior of the C200 GRPC in this paper, which is also employed by Klepaczko and Brara [20].

2. Experimental

2.1. Raw materials

Four types of cementitious materials are used in this study: Portland cement (PC) with 28 days of compressive strength of 68.9 MPa, Silica Fume (SF), Ultra Fine Fly Ash (UFFA), and Ultra Fine Slag (UFSL). Their chemical compositions and physical properties are given in Table 1.

The natural river sand with the maximum size of 3 mm is used in this study to replace the ultra fine quartz sand, which is a necessary component to produce RPC reported by published literatures. The superplasticizer with the water reducing ratio of 35% produced by Cika Company in Guangzhou, PR China is used. Steel fibers is specially designed and manufactured by Guo Mao Steel Fiber Company in Jiang Xi Province, PR China. The characteristic parameters of the steel fibers are: length (l_f) = 13 mm, diameter (d_f) = 0.175 mm, tensile strength = 1800–2000 MPa.

2.2. Mixture proportions of GRPC

Three different GRPC matrices (M1, M2 and M3) are designed. Their compositions are listed in Table 2. Portland cement (50–60%) is replaced by binary or ternary mineral admixtures of fly ash, slag and silica fume. Ultra fine quartz sand is totally replaced by natural river sand. In order to investigate the effect of steel fiber content on the quasi-static and dynamic mechanical properties of GRPC, the volume fraction (V_f) of steel fibers is varied from 0%, 2–4%.

2.3. Specimens preparation and curing

2.3.1. Specimens preparation

The cementitious materials (Portland cement and composite mineral admixtures) and river sand are first dry-mixed for 1 min. Then the water and superplasticizer are put into the pre-mixed powders and mixed for another 3 min. Finally, fiber is added into the mixture and mixed for 3 min so that fibers are homogenously distributed throughout the fresh mortar. After that, the fresh GRPC paste is cast into steel moulds and compacted using a vibrating table. The specimens are stored in the conditions (20 °C, 100% RH) for 24 h, then removed from the moulds, and cured in different curing regimes described in Section 2.3.2.

2.3.2. Curing

Three types of curing regimes are employed in the study:

(1) Standard curing (curing 1): 20 °C and 100% RH for 28 days.
(2) Steam curing (curing 2): 90 °C and RH = 100% for 24 h.
(3) Autoclave curing (curing 3): 200 °C and 1.7 MPa pressure for 8 h.

2.4. Testing methods

2.4.1. Fiber–GRPC matrix interfacial bonding strength

"Dumbbell" shaped specimen, as shown in Fig. 1, is prepared to measure the fiber–GRPC matrix interfacial bonding strength according to the Chinese standard testing method for steel fiber reinforced mortar. Nine fibers with the proportional spacing are placed in the middle section of the fresh GRPC matrix along the longitude direction. The average interfacial bonding strength is calculated for nine fibers.

2.4.2. Flexural, compressive and tensile strength

Specimens for flexural and compressive tests are 40 mm × 40 mm × 160 mm prisms. Flexural strength and compressive strength are tested according to GB177-85. At first, the three-point bending test is performed to obtain flexural strength. After bending test, the broken specimens with sizes of approximately 40 mm × 40 mm × 80 mm are used to conduct compressive test. Three samples of each batch are tested. The average value is served as the finial flexural strength and compressive strength. A closed-loop

Table 1
Chemical composition and physical properties of the four cementitious materials

Chemical compositions (%)	PC	SF	UFFA	UFSL
SiO_2	20.6	94.5	55.0	34.2
Fe_2O_3	4.4	0.8	5.9	0.4
MgO	0.6	1.0	1.3	6.7
Al_2O_3	5.0	0.3	31.3	14.2
CaO	65.1	0.5	3.9	41.7
SO_3	2.2	0.8	1.5	1.0
LOI	1.3	1.0	1.0	1.7
Specific surface area (m^2/kg)	417	2200	686	766

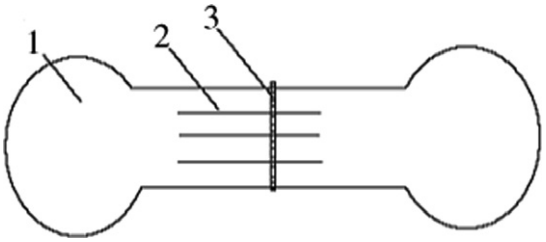

Fig. 1. Interfacial bonding strength testing specimen.

Table 2
Compositions of the three GRPC matrices

No.	PC (%)	SF (%)	UFFA (%)	UFSL (%)	Superplasticizer (%)	W/B	Binder to sand ratio
M1	50	0	25	25	1.7	0.15	1.2
M2	50	10	0	40	1.7	0.15	1.2
M3	40	10	25	25	1.7	0.15	1.2

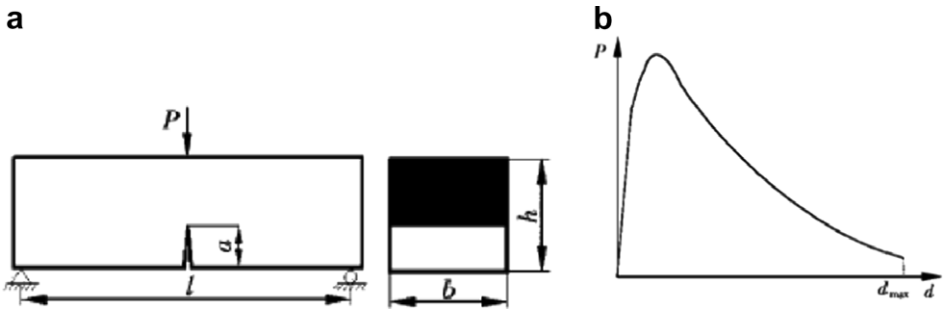

Fig. 2. Schematic diagram of fracture energy test.

servohydraulically controlled materials testing machine (Sintech 10/D MTS 810) is used to conduct flexural and compressive tests.

As for tensile strength, similar method for measuring the fiber–GRPC matrix interfacial bonding strength is employed. The direct tensile test is performed on the "dumbbell" shaped specimen using MTS 810 testing machine. Six specimens are prepared for each batch. The average value is used as the final tensile strength.

2.4.3. Fracture energy

The fracture energy can be obtained through three-point bending test for the beam with a notch, as shown in Fig. 2. The specimen (40 mm × 40 mm × 160 mm) with a cave of 15 mm depth in the middle is used in this study. The testing span is 150 mm and the rate of deformation is 0.02 mm/min. The fracture energy G is given by the following equation

$$G = \frac{\int_0^{\delta \max} P d\delta + \frac{1}{2} mg\delta \max}{(h-a)b} \quad (1)$$

where $\int_0^{\delta \max} P d\delta$ is the work of load P; $\frac{1}{2} mg\delta$ max is the work of specimen weight; m is the mass of a specimen; δ is the deformation; b and h are the width and height of a specimen, and a is the depth of the notch. In this test, $b = h = 40$ mm, $a = 15$ mm.

2.4.4. Dynamic tensile test

Dynamic tensile test is performed by using SHPB setup on cylinder specimen with 70 mm in diameter and 500 mm in length. The ends of all specimens are carefully grounded in order to assure the parallelism of the end surfaces. A typical SHPB setup to study the dynamic behavior of concrete is outlined in Fig. 3. It is composed of gas launcher, projectile, Hopkinson bar and long specimen. The projectile impact on the Hopkinson bar develops a compressive longitudinal incident wave. The incident wave is then transmitted into the concrete specimen, and a small part is reflected back to the Hopkinson bar due to the difference of impedances. The compressive wave that is transmitted into the specimen is reflected by the specimen free end as a tensile wave. The superposition of the incident compressive wave and the reflected tensile one, generates a tensile stress that grows rapidly in time along the concrete specimen. Due to the wave superposition, the net tensile wave leads to spalling (tensile fracture) of the concrete specimen at a certain distance from the free end, where the tensile stress reaches the critical value. The whole process of wave propagation is recorded via the three strain gauges cemented to the Hopkinson bar surface at three specified distances. This arrangement allows for determination of the fracture stress caused by spalling, the stress history in the specimen, the critical time of loading, and the loading rate or strain rate. Dynamic tensile test is performed on C200 GRPC with impact velocity between 4.0 m/s and 14 m/s. For each impact velocity, six specimens are tested.

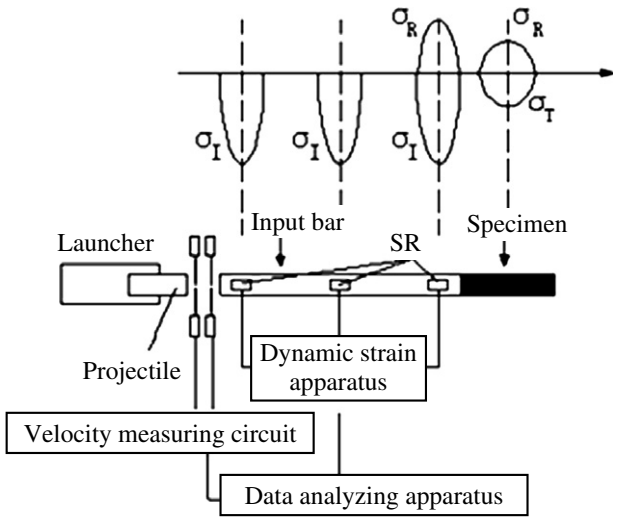

Fig. 3. Schematic diagram of SHPB for dynamic tensile test.

3. Results and discussion

3.1. Static mechanical properties of C200 GRPC

3.1.1. Compressive strength

The compressive strengths of various GRPCs made with different matrices, fiber content, curing regimes and curing ages are measured and given in Fig. 4a–d. As can be seen in Fig. 4a, the types of matrices have an important influence on the compressive strength. Comparing the three types of matrices (M1, M2, and M3), it can be observed that the matrix M3 incorporated with three kinds of ultra fine mineral admixtures (silica fume, fly ash, and slag) at the same time exhibits the highest compressive strength amongst the three types of matrices, whose compressive strengths reach 141.1, 155.0, and 158.0 MPa, respectively for matrix M3 prepared under curing 1, curing 2, and curing 3. In addition, the incorporation of small sized steel fiber, especially in the case of high volume fraction of fiber, evidently improves the compressive strength of GRPC in various curing regimes, as shown in Fig. 4b. The GRPCs with 4% fiber have approximately 30–50 MPa increase compared to the GRPC matrices without fiber. As a result, the compressive strength of GRPCs can reach 200 MPa under curing 1 for 180 days, or curing 2 or curing 3.

Considering the standard curing regime, i.e. curing 1 (20 °C, 100% RH) is a gentler curing regime than curing 2 and curing 3, the hydration reaction will continue to progress with the development of curing ages in a long period. In order to investigate the effect of curing ages, the compressive strength of various GRPCs are determined at ages of 28 days, 90 days, and 180 days, and displayed in Fig. 4c. It can be seen that the compressive strength has

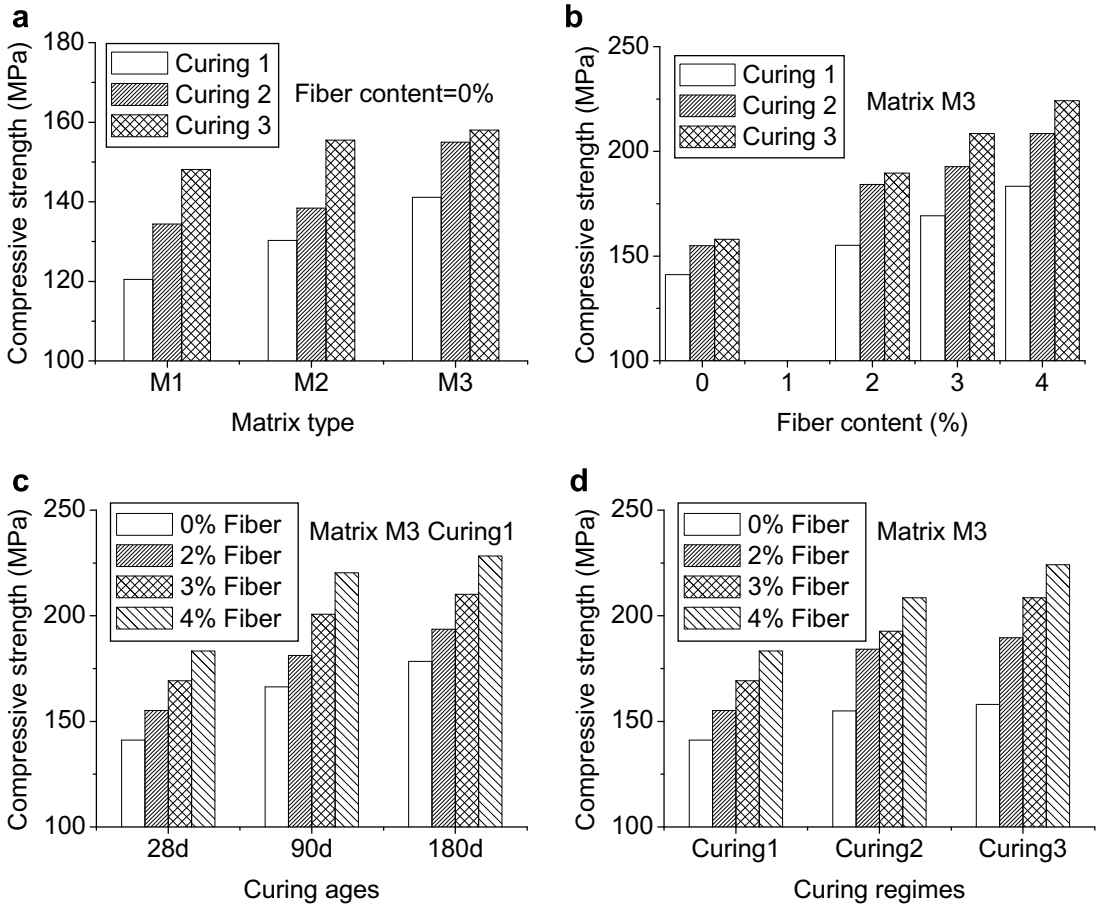

Fig. 4. Effect of types of matrices, fiber content, curing regimes and curing ages on compressive strength of GRPC.

an obvious increase for various GRPCs when curing age increases from 28 days to 90 days. After 90 days, the further prolonging of curing age shows a relatively little strength gain. For example, the compressive strengths of matrix M3 GRPC with 4% fiber are 183.3, 220.3, and 228.3 MPa at an age of 28, 90, and 180 days, respectively. There is a 37 MPa strength gain when curing age increases from 28 days to 90 days, while only 8 MPa gain from 90 days to 180 days. Thus, from the viewpoint of time and energy saving 90 days of curing ages is enough to achieve most of the ultimate strength.

The effects of different curing regimes are also investigated on compressive strength, as shown in Fig. 4d. As can be seen, GRPC under standard curing regime has the lowest strength. However, when steam curing is employed, compressive strength shows an obvious increase. Through 24-hour steam curing, about 15–30 MPa compressive strength is further gained when compared to the 28-day standard curing. Autoclave curing shows more attractive strength enhancement than stream curing. It is only through 8-hour autoclave curing that over 200 MPa compressive strength is achieved for various GRPCs with 3% or 4% fiber. The above analysis indicates that elevating temperatures can significantly increase the hydration rate, accelerate rapid formation of hydration products, resulting in high early strength. Although autoclave curing is most effective in improving compressive strength among three types of curing regimes, its high energy consumption and complex operation limit the curing regime to be extensively applied in practical engineering. Comparatively standard curing has such advantages as easy operation and lower energy consumption. If the curing ages is reasonably prolonged, 200 MPa compressive strength can also be achieved.

On basis of the above analysis, the GRPC with the compressive strength of 200 MPa or greater can be obtained by using 60 wt.% of ternary composite mineral admixtures consisting of 10% silica fume, 25% fly ash and 25% slag; utilizing natural sand to totally replace ultra fine quartz powder; incorporating 3–4% volume fraction of specially designed fine steel fiber; and employing 20 °C, 100% RH of curing condition for 90 days. Compared to the RPC commonly used across the world, the preparation of GRPC is cheaper, practical and easier. The advantages will make GRPC exhibit great potentials in the fields of civil engineering, military engineering, and nuclear waste treatment.

3.1.2. Flexural strength

The flexural strengths of various GRPCs are shown in Fig. 5(a–d). As can be seen, the effects of matrix types, fiber content, curing regimes and curing ages on the flexural strength of various GRPCs show a similar tendency as compressive strength, but larger effect is true to flexural strength when compared to compressive strength. The GRPC made with matrix M3 and 4% fiber can gain 60 MPa flexural strength under standard curing for 90 days.

3.1.3. Fracture energy

The fracture energy is an important parameter to describe the resistance to cracking and deforming. The fracture energy of various GRPCs under curing 2 and curing 3 is determined and depicted in Fig. 6. It can be seen from Fig. 6 that the fracture energy exhibits a sharp increase when small sized steel fiber is incorporated. Comparatively, the fiber content, curing regimes and types of matrices have a little influence on the fracture energy. For example, the fracture energy reaches 31,300 J/m^2 for GRPC with 3% volume fraction

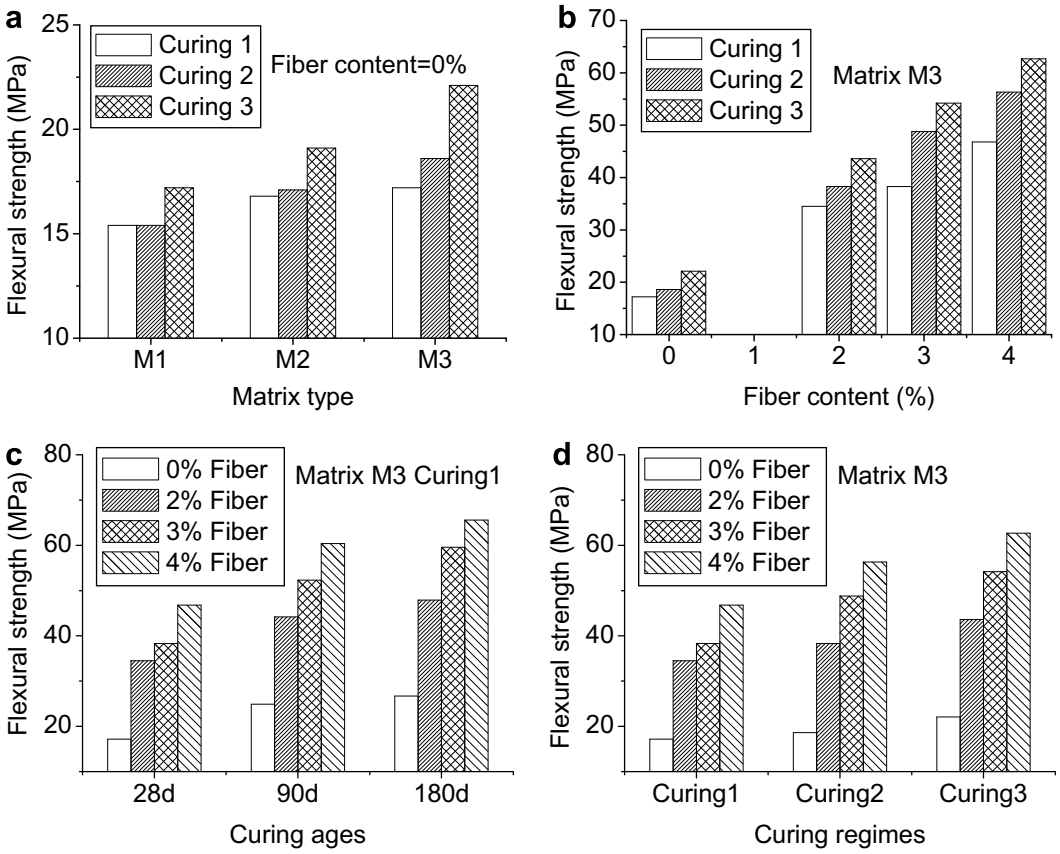

Fig. 5. Effect of types of matrices, fiber content, curing regimes and curing ages on flexural strength of GRPC.

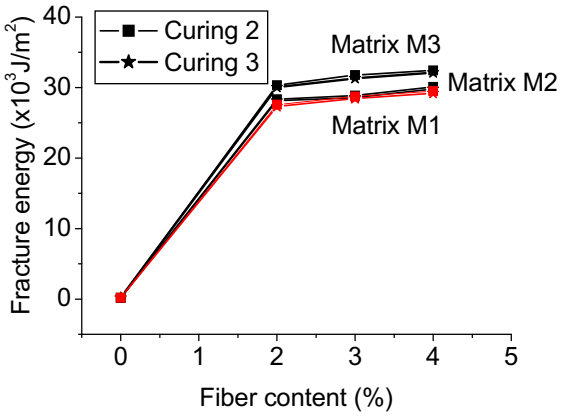

Fig. 6. Fracture energy of various GRPCs prepared under different curing regimes.

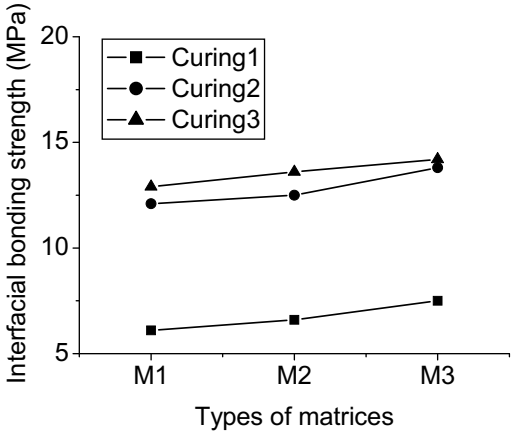

Fig. 7. Interfacial bonding strength between fiber and various GRPC matrices.

of fiber, while only 0.183 J/m^2 for GRPC without fiber. When the fiber volume fraction increases from 3% to 4%, the fracture energy only has an 800 J/m^2 gain.

3.1.4. Interfacial bonding strength

The interfacial bonding strength is one of the important indices to evaluate the bonding property between fibers and matrix. Generally, higher fiber–matrix interfacial bonding strength is expected for higher flexural and tensile strengths. The experimental results are shown in Fig. 7. As can be seen in Fig. 7, the types of matrices and the curing regimes, especially for the latter, have a significant impact on the fiber–matrix interfacial bonding strength. The interfacial bonding strength follows the order: M3 > M2 > M1 and curing 3 > curing 2 > curing 1. M3 matrix cured under curing 3 can gain the highest interfacial bonding strength, which is14.2 MPa.

3.2. Dynamic tensile behavior of C200 GRPC

Based on the experimental results of static mechanical tests, it can be conclude that M3 matrix exhibits superior mechanical properties (compressive, flexural strengths, fracture energy, and interfacial bonding) to M1 and M2 matrices. Thus, it is chosen as the optimum C200 GRPC matrix and is used to conduct the dynamic tensile test.

In order to determine the dynamic tensile strength of C200 GRPC, different impact velocity is used in the range of 4–14 m/s.

Figs. 8–10 shows the tensile stress vs. time curve of C200 GRPC under different impact velocity. When performing the dynamic tensile test, the lowest impact velocity, i.e. 4 m/s is first employed, then gradually increase the impact velocity up to the highest impact velocity 14 m/s. Once one small visible crack is observed, the corresponding peak stress is recorded and served as the minimal dynamic tensile strength. Table 3 shows the peak stress at different impact velocity. The minimal dynamic tensile strength is also marked with asterisk, as shown in Table 3. For the purpose of the comparison, the corresponding quasi-static tensile strength is also given in Table 3. In addition, the photos of the C200 GRPC are also taken after dynamic tensile tests, as shown in Fig. 11. Results show that: ① the dynamic tensile strength increases obviously with an increase of impact velocity, which shows high strain rate sensitivity. ② the minimal dynamic tensile strength is higher than quasi-static strength, especially for the GRPCs with high fiber content. ③ the incorporation of steel fiber shows an obvious strength improvement on GRPC matrix. The dynamic tensile strength of fiber reinforced GRPC is much larger than that of GRPC matrix without fiber. The failure characteristic of GRPC with fiber is totally different from that of GRPC matrix without fiber: the failure surface is very coarse and zigzag for GRPC with fiber. In contrast, a flat surface can be clearly seen for GRPC matrix without fiber. Furthermore, the damage of RPC matrix is also more serious than that of fiber reinforced ones under the same impact velocity.

3.3. Mechanism of excellent static and dynamic properties gains of C200 GRPC

The above static and dynamic tests show C200 GRPC made with 50–60% composite mineral admixtures, natural river sand and standard curing regime (20 °C, 90% RH), possess excellent static and dynamic properties. The gains of these excellent properties are mainly attributed to two aspects: One is from the compacted matrix made with different types and amounts of ultra fine composite mineral admixtures such as silica fume, fly ash and slag. the other is from small sized steel fibers.

3.3.1. Contribution of GRPC matrix

The water-binder ratio of the GRPC matrix prepared in this study is very low, only 0.15, resulting in a very compacted paste after setting and hardening. In addition, 60 wt.% of composite mineral admixtures in cementitious matrix could not be ignored. During the process of microstructure formation, the compact packing and filling effect, the pozzolanic effect and micro-aggregate effect of the composite mineral admixtures make GRPC matrix denser, lower porosity and less macro-defects, as compared with the one without mineral admixture incorporation. These effects will further improve with the development of curing ages, especially in the case of standard curing regime (curing 1), which results in higher compressive and tensile strength gains when cured under curing 1 for 180 days than the ones cured under the other two curing regimes. It should be noted that the micro-aggregate effect of fly ash plays an important role at later stages. It is because only about 20% of the total fly ash that will takes part in pozzolanic reaction, the remaining fly ash particles act as micro-aggregates

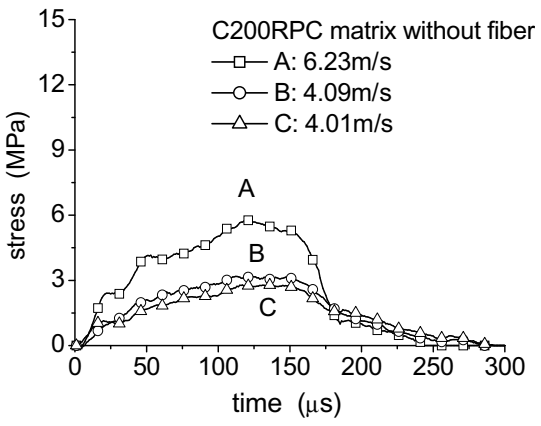

Fig. 8. Dynamic tensile stress–time curves of C200 GRPC matrix without fiber.

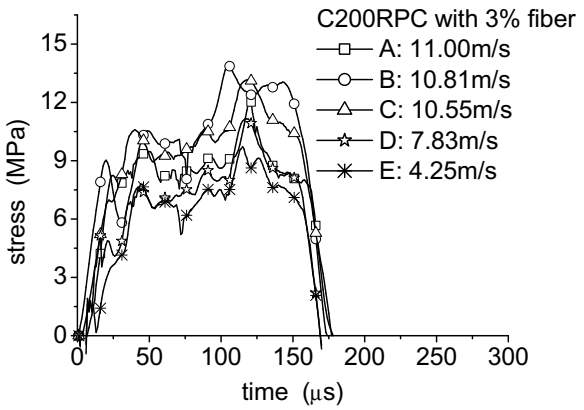

Fig. 9. Dynamic tensile stress–time curves of C200 GRPC with 3% fiber.

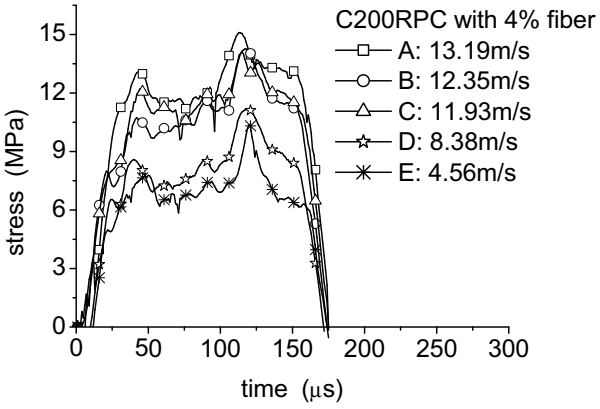

Fig. 10. Dynamic tensile stress–time curves of C200 GRPC with 4% fiber.

Table 3
Dynamic tensile experimental results of C200 GRPC with and without fiber

Types of GRPCs	Dynamic tensile strength		Static tensile strength (MPa)
	Impact speed (m/s)	Peak strength (MPa)	
C200 GRPC matrix	6.23	5.83*	5.0
	4.09	3.18	
	4.01	2.79	
C200 GRPC with 3% fiber	11.00	13.92*	9.7
	10.81	13.17	
	10.55	12.07	
	7.83	11.16	
	4.25	9.72	
C200 GRPC with 4% fiber	13.19	15.11	10.2
	12.35	14.26*	
	11.93	14.12	
	8.38	11.17	
	4.56	10.37	

Note: The minimum dynamic tensile strength is marked with* asterisk.

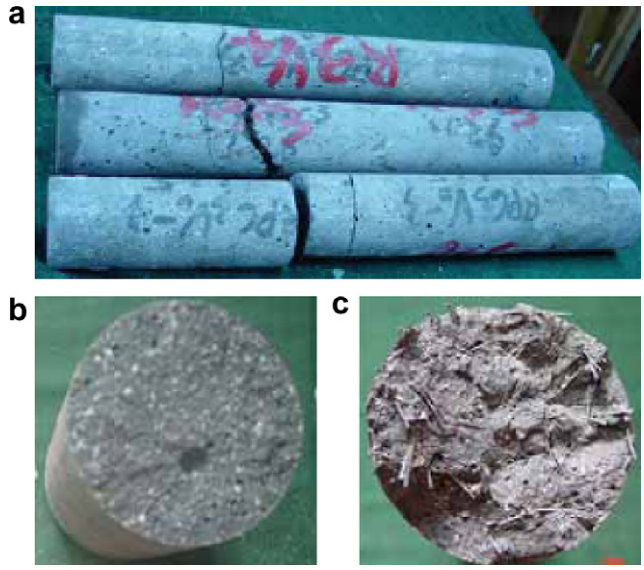

Fig. 11. Failure photos of C200 GRPCs with and without fiber after dynamic tensile test.

Table 4
Fiber numbers per unit meter and average spacing of GRPC [26]

Fiber size	l_f = 13 mm, d_f = 0.175 mm		
Volume fraction (%)	2	3	4
Fiber numbers (N/m^3)	6.40×10^7	9.60×10^7	1.28×10^8
Fiber average spacing (mm)	1.55	1.26	1.09

[24]. In addition, the high hardness and elastic modulus of fly ash particles can efficiently reduce the distortion and micro-cracking of GRPC's matrix, which is another reason for the achievement of the excellent static and dynamic properties of GRPC [25].

3.3.2. Contribution of steel fibers

Steel fiber can greatly increase flexural and tensile strengths, improve toughness and reduce cracking. The advantageous effects mainly depend on the fiber volume fraction and size. The greater the volume fraction and the less the size of steel fibers, the greater the static and dynamic mechanical strengths will be. In this paper, a type of small sized steel fiber is specially designed and used to reinforce GRPC matrix. The average numbers and spacing of steel fibers in GRPC with different fiber content are calculated and listed in Table 4. It can be seen that the fiber numbers are 6.4×10^7, 9.6×10^7, 1.28×10^8 pieces/m^3, respectively for the GRPCs with 2% fiber, 3% fiber and 4% fiber. The corresponding average fiber spacing is 1.55 mm, 1.26 mm and 1.09 mm, respectively. Compared to the normal steel fiber reinforced concrete, the fiber numbers are one or two order of magnitude greater for GRPC, and the fiber average spacing is two or four times larger, thus a great increase in static and dynamic strengths.

4. Conclusions

(1) A novel type of green reactive powder concrete with compressive strength of 200 MPa (C200 GRPC) is successfully prepared in this study by utilizing composite mineral admixtures consisting of 10% silica fume, 25% fly ash and 25% slag to replace 50–60 wt.% of Portland cement, using natural river sand with the maximal diameter of 3 mm to totally replace the ultra fine quartz sand with the maximal diameter of 600 μm, incorporating 3–4% volume fraction of small sized steel fibers, and employing low energy consumption curing regime-20 °C and 100% RH for 90 days. The C200 GRPC has many advantages over commonly used C200 RPC such as the low production cost, less energy consumption, easier operation, which make C200 GRPC have great potentials in the fields of civil, pavement, bridge and military engineering.

(2) The static mechanical behaviors (mechanical strength, fracture energy and interfacial bonding strength) of various GRPCs with different matrices, fiber content, curing regimes and curing ages is systematically investigated. The results show that the matrix M3 incorporated with three kinds of ultra fine mineral admixtures (silica fume, fly ash and slag) at the same time exhibits the highest mechanical strength amongst the three types of matrices (M1, M2, and M3). The incorporation of small sized steel fiber, especially in the case of high volume fraction of fiber, greatly improves the static mechanical strengths of various GRPCs. Curing regimes and curing ages also have a great impact on the static mechanical behaviors. Elevating temperatures and prolonging curing ages can significantly increase the hydration rate, accelerate rapid formation of hydration products, resulting in high early strength. However, too high curing temperature will lead to high energy consumption and complex operation, thus a relative gentle curing regime-20 °C and 100% RH for 90 days is employed to prepare C200 GRPC.

(3) Strain rate has an important effect on the dynamic performance of RPC. With an increase of strain rate, GRPC's peak stress rapidly increases. The incorporation of steel fibers greatly reduces the damage degree of GRPC under high speed impact.

(4) The excellent static and dynamic properties of GPRC are mainly ascribed to two aspects: One is the ultra fine steel fiber involving its large numbers, small average spacing. This greatly improves the GRPC's mechanical strength, fracture energy and interfacial bonding strength. The second aspect is attributed to the particle packing and filling effect, the pozzolanic effect and micro-aggregate effect of the composite mineral admixtures, resulting in a very compacted GRPC matrix with low porosity and little macro-defects. these effects will further improve with the development of curing ages under standard curing regime.

Acknowledgements

Authors gratefully acknowledge the financial support from China National Natural Science Foundation (50702014), Project (A1420060186); Outstanding Young Teacher's Teaching and Researching Plan from Southeast University; West Project (2006ZB12) from Ministry of Communications of China; and Jiangsu Province Qinglan project.

References

[1] Richard P, Cheyrezy M. Reactive powder concrete with high ductility and 200–800 MPa compressive strength. ACI SP 1994;144:507–18.
[2] Bonneau Olivier, Lachemi Mohamed, Dallaire Eric, et al. Mechanical properties and durability of two industrial reactive powder concretes. ACI Mater J 1997;94(4):286–90.
[3] Matte V, Moranville M. Durability of reactive powder composites: influence of silica fume on the leaching properties of very low water/binder pastes. Cement Concrete Comp 1999;21(1):1–9.
[4] Allan CLW, Paul AC, Richard B, et al. Simultaneous measurement of shrinkage and temperature of reactive powder concrete at early-age using fiber Bragg grating sensors. Cement Concrete Comp 2007;29(60):490–7.
[5] Cheyrezy M, Maret V, Frouin L. Microstructural analysis of reactive powder concrete. Cement Concrete Res 1995;25(7):1491–500.

[6] Zanni H, Cheyrezy M, Maret V, Philippot S, Nieto P. Investigation of hydration and pozzolanic reaction in reactive powder concrete (RPC) using 29Si NMR. Cement Concrete Res 1996;26(1):93–100.
[7] Feylessoufi A, Villieras F, Michot LJ, De Donato P, Cases JM. Water environment and nanostructural network in a reactive powder concrete. Cement Concrete Comp 1996;18(1):23–9.
[8] Reda MM, Shrive NG, Gillott JE. Microstructural investigation of innovative UHPC. Cement Concrete Res 1999;29(3):323–9.
[9] Bonneau O, Vernetb C, Moranville M, Aïtcin P-C. Characterization of the granular packing and percolation threshold of reactive powder concrete. Cement Concrete Res 2000;30(12):1861–7.
[10] Matte V, Moranville M, Adenot F, Richet C, Torrenti JM. Simulated microstructure and transport properties of ultra-high performance cement-based materials. Cement Concrete Res 2000;30(12):1947–54.
[11] Morin V, Cohen-Tenoudji F, Feylessoufi A, Richard P. Evolution of the capillary network in a reactive powder concrete during hydration process. Cement Concrete Res 2002;32(2):1907–14.
[12] Pierre-Claude Aïtcin. Cements of yesterday and today: concrete of tomorrow. Cement Concrete Res 2000;30(9):1349–59.
[13] Cyr MF, Shah SP. Advances in concrete technology. In: Proceedings of the international conference on advances in building technology, 4–6 December, Hong Kong, China; 2002. p. 17–27.
[14] Ming GL, Yung CW, Chui TC. A preliminary study of reactive powder concrete as a new repair material. Constr Build Mater 2007;21(1):182–9.
[15] Bonneau Oliver, Poulin Claude, Dugat Jerome, et al. Reactive powder concretes: from theory to practice. Concrete Int 1996;18(4):47–9.
[16] Cheyrezy Marcel. Structural applications of RPC. Concrete 1999;33(1):20–3.
[17] Richard Pierre, Cheyrezy Marcel. Composition of reactive powder concrete. Cement Concrete Res 1995;25(7):1501–11.
[18] Feylessoufi A, Crespin M, Dion P, Bergaya F, Van Damme H, Richard P. Controlled rate thermal treatment of reactive powder concretes. Adv Cement Based Mater 1997;6(1):21–7.
[19] Halit Yazıcı. The effect of curing conditions on compressive strength of ultra high strength concrete with high volume mineral admixtures. Build Environ 2007;42(5):2083–9.
[20] Klepaczko JR, Brara A. An experimental method for dynamic tensile testing of concrete by spalling. Int J Impact Eng 2001;25(4):387–409.
[21] Galvez Diaz-Rubio F, Rodriguez Perez J, Sanchez Galvez V. The spalling of long bars as a reliable method of measuring the dynamic tensile strength of ceramics. Int J Impact Eng 2002;27(2):161–77.
[22] Chen W, Lu F, Cheng M. Tension and compression tests of two polymers under quasi-static and dynamic loading. Polym Test 2002;21(2):113–21.
[23] Jiao Chujie. Study on behavior of HPSFRC and UHPSFRC subjected to impact and blast. Doctorial thesis, Southeast University, Nanjing, China; 2004.
[24] Zhang Yunsheng, Sun Wei, Zheng Keren, Jia Yantao. Hydration process of Portland cement-fly ash pastes. J Southeast University (Nat Sci Ed) 2006;36(1):118–23.
[25] Zhao Qingxin, Sun Wei, Zhen Keren, Jiang Guoqing. Comparison for elastic modulus of cement, ground granulated blast furnace slag and fly ash particles. J Chin Cerm Soc 2005;33(7):837–41.
[26] Romualdi JP, Mandel JA. Tensile strength of concrete affected by uniformly dispersed and closely spaced short length of wire reinforcement. ACI J Proc 1964;61(6):657–71.